Monotonic and Cyclic Lateral Tests on Driven Piles in Chalk

F Ciavaglia[+], J Carey[+], A Diambra[*]

[+] *Wind Support Ltd, Bath, United Kingdom*

[*] *University of Bristol, Bristol, United Kingdom*

Revised technical paper submitted for possible publication to:

ICE Geotechnical Engineering

on 19/12/2016

Paper category: Technical Paper

Author to receive correspondence: Dr Andrea Diambra

Lecturer in Geomechanics
Queen's School of Engineering
University of Bristol
Bristol (UK)
andrea.diambra@bristol.ac.uk

Number of words: approx. 4880.

Number of tables: 4

Number of figures: 18

ABSTRACT

This paper describes the results of a pile testing campaign on open-ended tubular steel instrumented piles driven into chalk. The testing campaign comprised the performance of both monotonic and one-way cyclic lateral load tests, performed at different times after pile installation. The tests were performed on five piles with uniform outer diameters of 762 mm and embedded lengths of 4 m and 10 m, in order to investigate the difference in response between short and long piles.

Lateral pile head load–displacement behaviour to failure has been analysed. The tangent stiffness evolution during monotonic loading has been evaluated at different times after pile installation and the chalk set-up has been found to have no effect on piles behaviour under lateral loading. The pile secant stiffness during cyclic lateral loading is also investigated. Accumulated pile head lateral displacements are discussed and their pattern is described by a logarithmic function that varies with number of cycles. The creation of a gap between the chalk and the pile during cyclic lateral loading was observed, which influenced the shape of the load-displacement loops. The influence of the instrument protection system was taken into account in analysing the results.

1 INTRODUCTION

Chalk is a widespread geomaterial across the east and south eastern areas of the UK, the southern North Sea, the English Channel and the Baltic. Onshore and offshore wind farms are being developed in these areas. Driven steel piles are the foundation choice for most offshore wind turbines, but unfortunately, there are no established proven methods for analysing the lateral loading behaviour of driven piles in chalk. This is because very few piles tests have been carried out on piles in chalk, especially on driven piles. These limitations are reflected in CIRIA C574 (Lord *et al*., 2002), which represents the current state-of-the-art of engineering in chalk. Prior to this research project, only one single set of test results had been published for a laterally loaded driven pile in

chalk (Lord and Davies, 1979). This pile was an 800mm diameter open-ended tubular steel pile, driven to 4m depth. The chalk was characterised by Lord and Davies as "Grade II" using the old Mundford system, which is defined as "blocky medium-hard chalk with joints more than 200 mm apart and closed". This material is comparable to "medium to high density Grade A1" under the CIRIA C574 classification system. Lord and Davies suggested that the driving process damaged the surrounding material to become a structureless remoulded chalk containing small lumps of intact chalk. Indeed, the design of laterally loaded pile in chalk is complicated by the uncertainty of how pile driving affects the lateral-load response of the chalk

This paper aims to contribute to the advancement of the limited understanding on the behaviour of driven piles in chalk when subject to lateral loading, in order to help the development of current and future design methodologies. The pile testing campaign included the performance of both monotonic and one-way cyclic lateral loading tests on five open ended steel tubular piles. Pile test results related to initial pile lateral stiffness, ultimate lateral resistance, stiffness degradation due to cyclic loading, and set-up effects are discussed in the following.

2 TEST SITE AND GROUND CONDITIONS

The test site is in a disused chalk pit located in St Nicholas-at-Wade in Kent, Southern England (see Fig.1). The chalk pit was previously excavated for the development of the Thanet Way road embankment, and all the weathered chalk has been removed by the previous quarrying activity. The chalk has been classified as low to medium density CIRIA Grade A3 to B2, based on typical discontinuity apertures varying between closed (Grade A) and less than 3 mm (Grade B) and typical discontinuity spacing varying between 60mm and 600mm.

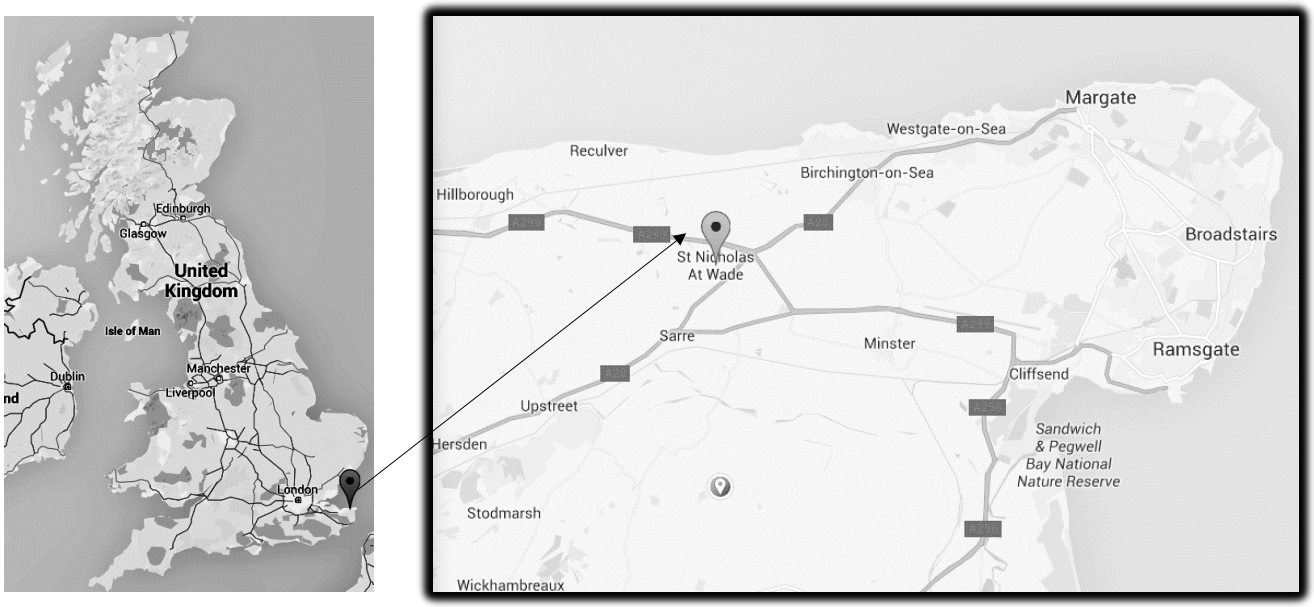

Fig.1. Location of Pile Testing Site (St. Nicholas at Wade, Kent, UK).

The site has been thoroughly characterised by two site investigations, one carried out in 2007 and one in 2011 (SEtech, 2007; Fugro, 2012a; Fugro, 2012b). A total number of five boreholes were drilled up to 20m depth and laboratory tests were undertaken on the chalk samples taken by rotary coring. Chalk core logging determined a succession of the Margate Chalk overlying the Seaford Chalk formation with a transition at about 7 m depth (Mortimore, 2007). A total number of nine cone penetration tests (CPT) were also performed to a depth of 11-20 m below ground level using a 20 tonne CPT truck. Two representative CPT profiles, performed on the exact location of two tested piles, are reported in Fig. 2. Additionally, two cyclic CPTs were performed on the same site and the results are presented in Diambra *et al.* (2014). The chalk was found to be generally within 0.5% of a fully saturated state, even though the groundwater level was about 10 to 11 m below the current ground level. Results from laboratory unconfined compression tests and from in-situ high pressure dilatometer indicated unconfined compressive strengths between 2.1 MPa and 3.3 MPa with a mean value of 2.4 MPa. A summary of the key properties of the chalk from the two site investigations are shown in Table 1.

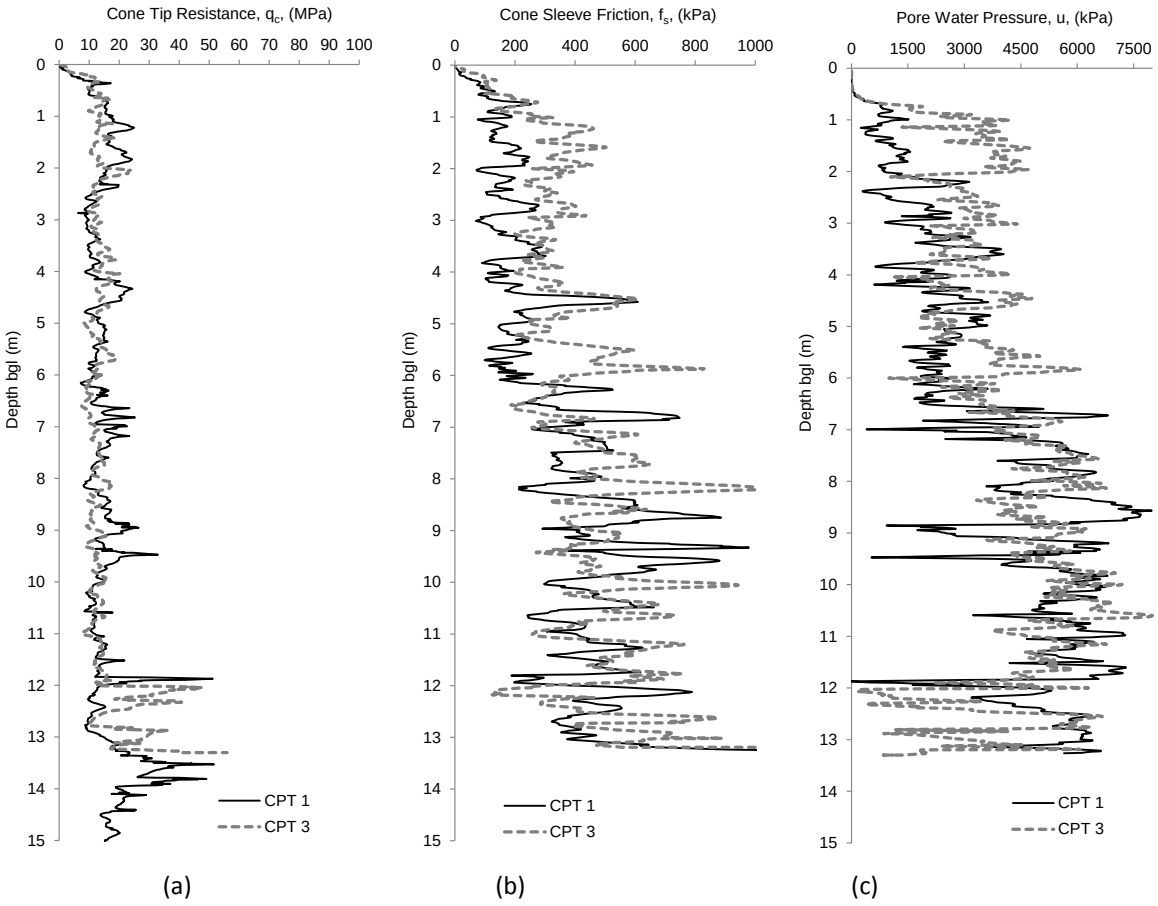

Fig. 2. Typical CPT log results including: (a) cone tip resistance (q_c); (b) sleeve friction (f_s) and (c) pore pressure. (u)

Table 1 - Key Properties of the Chalk at Test Site

Chalk Formation	Within the Margate chalk member and upper part of the Seaford Chalk Formation of the White Chalk Subgroup
CIRIA Grade	Low to Medium Density Grade A3 to B2
Dry Density (Mg/m^3)	Average 1.50 (Range 1.38-1.73)
Saturation Moisture Content (%)	29.5 (21-33)
Porosity (%)	44 (36-47)
Unconfined Compressive Strength, UCS, (MPa)	2.4 (2.1-3.3)

3 TEST PILE CONFIGURATION

3.1 PILE CHARACTERISTICS AND INSTRUMENTATION

The tests were performed on five open-ended tubular steel piles, labelled Pile 1 to Pile 5 in this paper. Piles 1, 2 and 3 are characterised by a total pile length (L) of 5 m and an embedded length (EL) of 4 m, whilst Piles 4 and 5 are 11 m long with an EL of 10. All the piles have an outside diameter (D) of 762 mm. Based on the deflected pile shape derived from pile instrumentation readings during lateral loading, Piles 1, 2 and 3 can be categorised as 'short' semi-rigid piles, and Piles 4 and 5 as 'long' flexible piles (Terzaghi *et al.*, 1996). Key dimensions of the five piles are summarised in Table 2. The pile steel grade is API 5L X65, which gives a yield stress in the region of 448 N/mm^2.

Table 2– Summary of Pile Characteristics and Instrumentation

Pile No.	1	2	3	4	5
Outer diameter (D)	762 mm	762 mm	762 mm	762 mm	762 mm
Wall thickness (WT)	44.5 mm	44.5 mm	44.5 mm	25.4 mm	25.4 mm
Total length (L)	5m	5m	5m	11 m	11 m
Embedded length (EL)	4m	4m	4m	10 m	10 m
Embedded length to diameter ratio (EL/D)	5	5	5	12.5	12.5
Expected pile behaviour	' Semi-rigid'	' Semi-rigid'	' Semi-rigid'	'Flexible'	'Flexible'
Vibrating wire strain gauges No.	20	20	20	28	/
Installed on	22 Nov. 2011	22 Nov. 2011	23 Nov. 2011	22 Nov. 2011	22 Nov. 2011
	16:15-17:00	14:55 -15:15	09:45-10:00	13:00 -13:35	14:00 -14:20

Linear Variable Displacement Transducers (LVDT) were attached to the top of the pile (Fig. 3a) in order to determine the pile head displacement (d) of the pile at the point of load application, 700 mm above the ground level. Piles 1 to 4 were instrumented with vibrating wire (VW) strain gauges (EDS 20 VA "surface-mount" type), attached to the outside wall of the pile by arc-welding and protected from damage during pile transportation and installation by four continuously welded angular steel channels (see Fig. 3b), closed at the pile toe using a 90 degree tapered steel

plate with a nominal height of approximately 100 mm. Four strain gauges were attached to the pile at selected depth, two in the direction of lateral load and two in the opposite direction. Results from strain gauges measurements have been used to determine shaft friction distribution during uplift pile tests (Ciavaglia et al., 2016) and to determine lateral p-y curves, which analysis is currently under development and outside the scope of this paper.

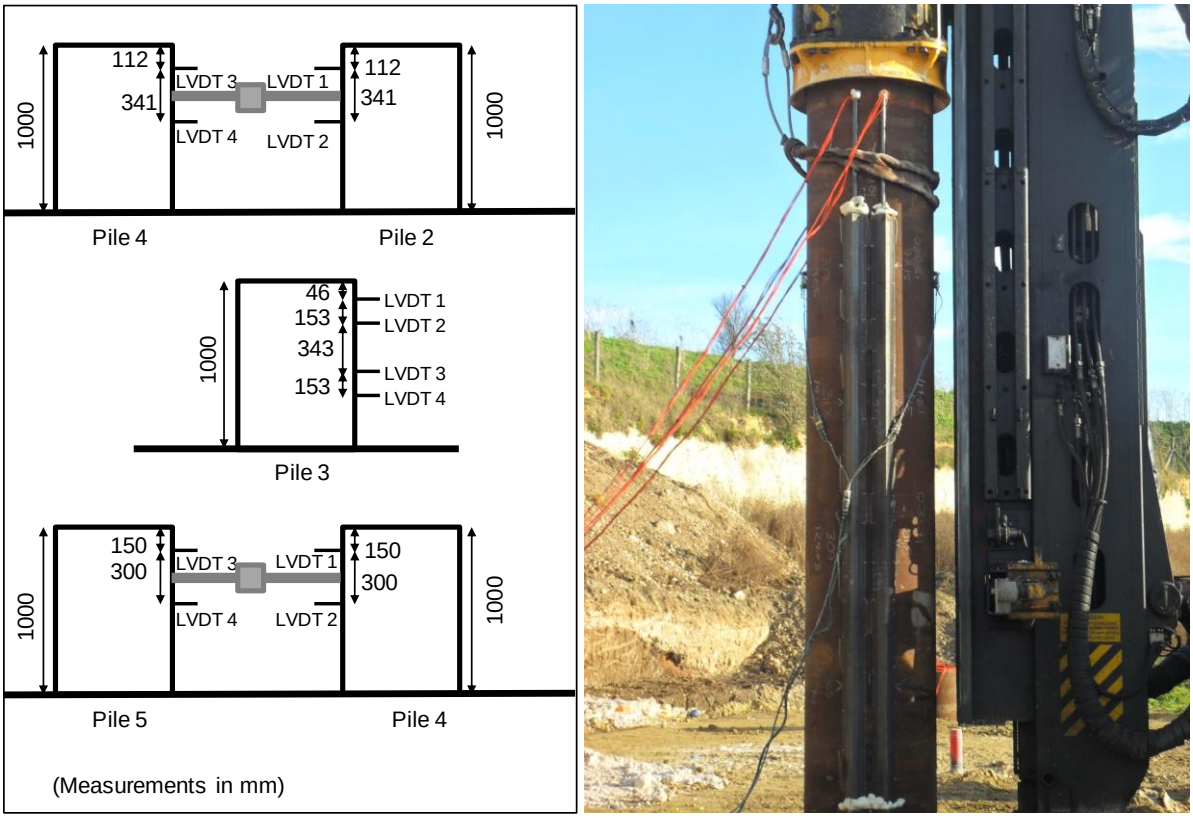

(a) (b)

Fig. 3. Piles Instrumentation: (a) LVDT Positions, (b) Pile Driving with view of Strain Gauges Angular Protection.

3.2 PILE INSTALLATION

The five piles were driven using a 7 tonne accelerated type hammer (7t Junttan PM 20). As expected, an annulus of remoulded chalk was created adjacent to the piles during driving. The thickness of this annulus was found to vary between 40%-50% of the pile wall thickness (see Fig. 4a) around all the piles, but a thicker zone of disturbed chalk was found in front of the strain gauge protection (see Fig 4b) with the instrumented piles. One of the piles (Pile 3) was partially exhumed

after the completion of the tests and the remoulded chalk annulus was visible adjacent to the pile shaft. Further details of the effects of pile driving are given in Ciavaglia *et al.* (2016).

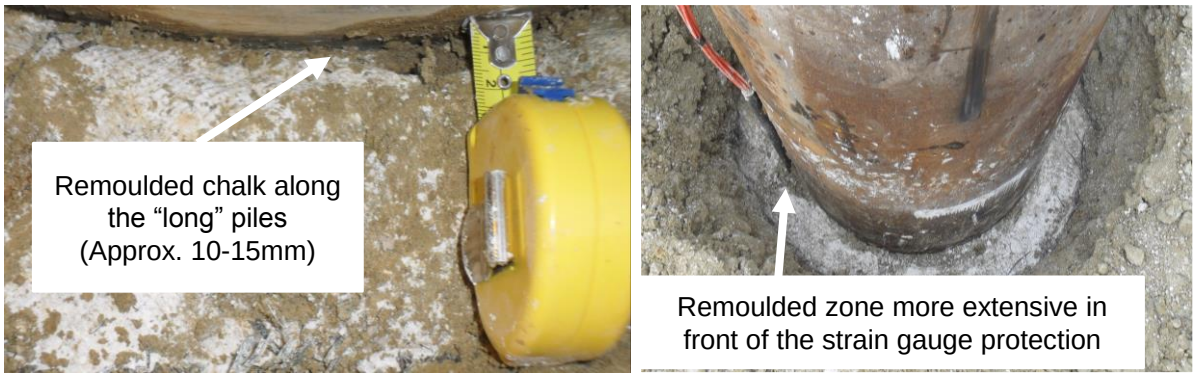

(a) (b)

Fig.4. Remoulded chalk annulus around the pile (a) close-up showing the dimensions and (b) around the pile including in front of the protection.

3.3 PILE LAYOUT AND TESTING STRATEGY

The layout of the piles after installation is provided in Fig. 5, where the locations of the boreholes and CPTs are also mapped. Piles 2 to 5 were subject to monotonic and cyclic lateral loading, while Pile 1 was subject to axial loading only, these results are presented and analysed separately in Ciavaglia *et al.* (2016). Direction of the lateral loading for the tests performed on each pile are also shown in Fig. 5. The minimum pile spacing (*s*) to pile diameter ratio in the direction of loading was about 10.5, which is thought to avoid any pile-to-pile interaction effect during lateral loading.

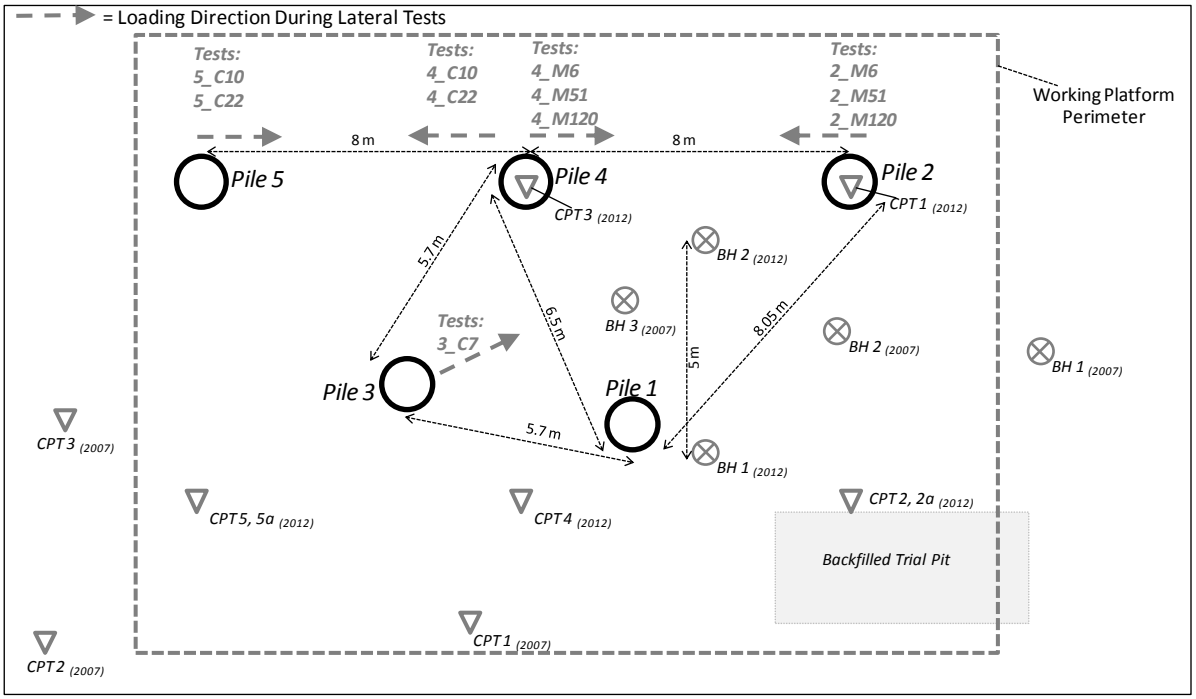

Fig.5. Test Pile Lay-out showing pile loading direction and borehole/CPT locations.

The monotonic and cyclic lateral loading tests were performed in three phases at different times after installation. Generally, the tests took place at 2-5 days, 7 weeks and 4 months after driving. A complete list of the performed tests and their details is provided in Table 3. The pile test codes used in the table, includes the pile number (2 to 5), the type of test ('M' for Monotonic and 'C' for Cyclic), and the number of days after pile driving when the tests were performed. For example, Test 2_M5 was carried out on Pile 2, applying a monotonic loading sequence and it was performed 5 days after installation.

The main purpose of the monotonic (M) test series (see Table 3) was to determine the evolution of the initial pile lateral stiffness at different times after pile installation on both short (Pile 2) on long (Pile 4) piles. It is well-known that "set-up" influences the axial behaviour of piles in chalk (Lord *et al*., 2002) but it is unknown if there is a similar effect on the lateral response. The main purpose of the cyclic tests on Pile 3 was to investigate the lateral load-displacement behaviour of a 'short' pile under cyclic loading, and to determine its post-cyclic ultimate lateral load capacity. Finally, cyclic

tests on the long Piles 4 and 5 were performed to investigate the response of long piles under cyclic conditions of progressively increased load levels.

Table 3. Summary of Performed Pile Tests

Pile No.	Test name	Time after driving (days)	Test type	Max load (kN)	Description
2	2_M6	6	Monotonic	220	Monotonic tests with unloading reloading loops at 40 kN, 80 kN and 220 kN
	2_M51	51	Monotonic	190	Monotonic tests with unloading reloading loops at 60 kN, 80 kN, 160 kN and190 kN
	2_M120	120	Monotonic	1260	Monotonic tests with unloading reloading loops at 80 kN, 160 kN, 220 kN and1260 kN
3	3_C7	7	Prog. Cyclic + Monotonic	1200/2346	Cyclic loading in Table 3 up to 1200 kN followed by monotonic loading to 2346 kN
4	4_M6	6	Monotonic	220	Monotonic tests with unloading reloading loops at 40 kN, 80 kN and 220 kN
	4_M51	51	Monotonic	190	Monotonic tests with unloading reloading loops at 60 kN, 80 kN, 160 kN and190 kN
	4_M120	120	Monotonic	1260	Monotonic tests with unloading reloading loops at 80 kN, 160 kN, 220 kN and1260 kN
	4_C10	10	Prog. Cyclic	800	Cyclic loading in Table 3 up to 800 kN
	4_C122	122	Prog. Cyclic + Monotonic	1500/2000	Cyclic loading in Table 3 up to 1500 kN followed by monotonic loading to 2000 kN
5	5_C10	10	Prog. Cyclic	800	Cyclic loading in Table 3 up to 800 kN
	5_C122	122	Prog. Cyclic + Monotonic	1500/2000	Cyclic loading in Table 3 up to 1500 kN followed by monotonic loading to 2000 kN

3.4 TESTING EQUIPMENT AND METHODOLOGY

The lateral load tests were performed by pushing or pulling the piles against each other using a hydraulic jack and a loading frame directly connected to the tested piles. The applied load was measured using a load cell, whilst the pile head movement was measured using the multiple Linear Variable Displacement Transducers (LVDTs) located at the top of the piles. For test series 2_M and 4_M, Piles 2 and 4 were pulled towards each other to provide mutual reaction forces (see Fig. 6). Test 3_C7 was undertaken using piles 1, 2 and 4 as a reaction, with the aid of the load spreader/support beam shown in Figure 6. For test series 4_C and 5-C, Piles 4 and 5 were pulled towards each other.

(a) (b)

Fig.6 - Lateral Test Apparatus: (a) used for Tests series 2_M and 4_M and (b) used for Test 3_C7

The LVDTs reading were taken every 12 seconds simultaneously for both piles pulled towards each other. Unload-reload loops were performed for 2 or 3 selected peak loads, the purpose of which was to measure the variations in reloading stiffness with peak load, and for investigating the influence of 'set-up' time on the reloading stiffness also. The maximum applied load during the tests (see Table 3) were selected in order to limit chalk disturbance for later tests.

The detailed loading sequence for the cyclic tests on Piles 3, 4 and 5 (tests 3_C7, 4_C10, 5_C10, 4_C122 and 5_C122) are reported in Table 4, which includes loading levels, numbers of cycles and average periods of each cycle. After completion of the cyclic loading stage the piles were subjected to monotonic loading to a higher load level whose maximum value is reported in Table 3.

Table 4. Details of Loading Stages for the Cyclic Tests

Test No.	Loading sequence No.	Cyclic load amplitude (kN)	Peak load (kN)	Number of cycles	Average cycle period (minutes)
3C_7	1	0-115	115	100	2-2.5
	2	50-100	100	100	1.4
	3	0-150	150	100	2
	4	0-250	250	100	1.2
	5	0-400	400	100	2
	6	400-800	800	20	3
	7	600-1200	1200	20	3
4C_10 & 5C_10	1	0-100	100	100	1.5
	2	0-250	250	45	2.4
	3	0-350	350	25	3
	4	0-500	500	20	3
	5	0-800	800	20	5
	6	400-800	800	10	4
4C_122 & 5C_122	1	0-300	300	50	1.5
	2	0-500	500	30	3
	3	400-800	800	30	2
	4	0-1000	1000	30	4
	5	600-1200	1200	20	3
	6	0-1500	1500	9	10

4 MONOTONIC LOADING TEST RESULTS

4.1 LARGE STRAIN DATA

Figure7 presents lateral load-displacement curves for the two 'short' Piles 2 and 3, (Tests 3_C7 and 2_M120 in Fig.7a) and for the two 'long' piles 4 and 5 (Tests 4_M120, 4_C10, 4_C122, 5_C10 and 5_C122 in Fig.7b). Tests 2_M6, 2_M51, 4_M6 and 4_M51 are not discussed in this section because they are only representative of a relatively low load level response. Two load-displacement curves are reported for Pile 4 in Fig.7b; one for the monotonic test 4_M120 and one for the cyclic test 4C_122, which were performed by pulling the pile in opposite directions.

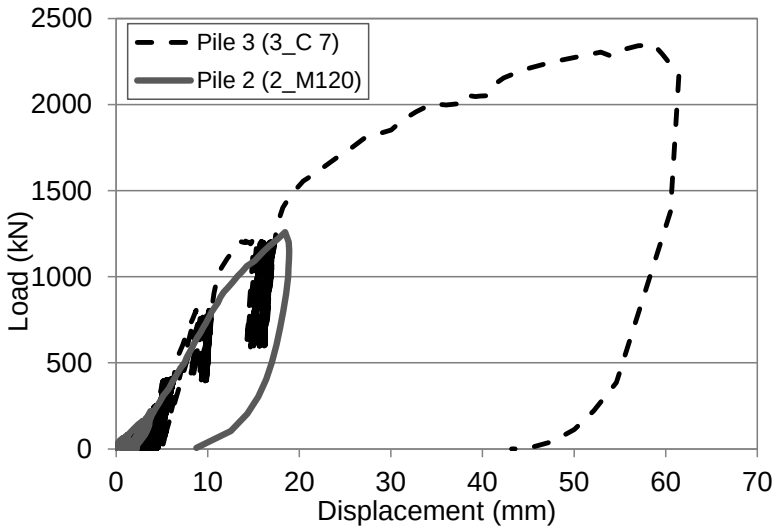

(a)

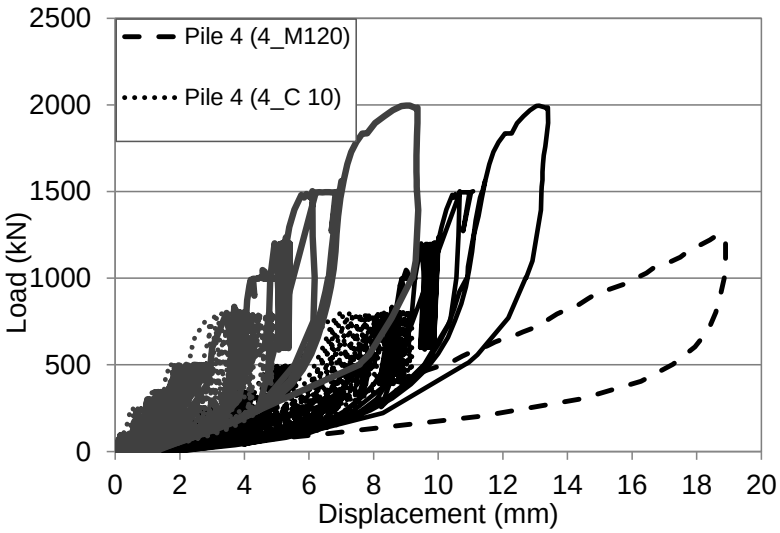

(b)

Fig. 7. Lateral Load vs Pile Head Displacement Response of 'Short' Piles 2 and 3 (a) and 'Long' Piles 4 and 5 (b).

Only the short piles could be brought to failure with the available capacity of the hydraulic jack. Failure is defined as the pile experiencing large additional displacements with only small increases in load. For the specific case of the 'short' pile, the excessive pile top displacement was associated with the failure of the surrounding chalk rather than failure of the pile steel.

A pile 'ultimate lateral resistance' of 2346 kN was recorded for Pile 3. The other 'short' Pile 2 was instead loaded only up to about 50% of this recorded ultimate capacity. Direct comparison of the load-displacement curve for the two piles shows that the loading envelope for Pile 3 is very similar to the monotonic loading curve for Pile 2 (Fig. 7a). This suggests that the cyclic loads applied to Pile 3 did not affect the general lateral load-displacement behaviour in a negative manner. It also gives some confidence in the reliability and repeatability of the results.

A different picture can be observed from the results on the 'long' Piles 4 and 5, which were loaded up to 2000 kN (Fig.7b). Direct comparison of the two lateral load tests performed on Pile 4 on opposite directions (Tests 4_M120 and 4_C10) suggests that the chalk conditions were different on opposite sides of Pile 4. The load-displacement curve obtained from Test 4_M120 appears much softer than the one obtained during Test 4_C122, suggesting a weaker or more fractured/weathered chalk state on the side of the former test. It should be noticed that before the start of each loading test, the area around the pile was flooded with water in order to increase the water content of the chalk towards full saturated conditions and it was noticed that water soaked more easily into the side of the pile where a softer behaviour was observed. This preferential flow path is likely linked to a higher amount of chalk fractures, which may be related to the inhomogeneity of either the original in situ condition or the disturbance caused by pile driving.

The stiffer response of Pile 5 than Pile 4 (Fig.7b) may be more likely ascribed to the absence of the strain gauge instrumentation system in front of Pile 5. The angular protection (Fig. 3b) represents a thickening of the pile wall by up to 130mm and its presence probably caused some additional chalk disturbance during the driving installation process. In Fig 4a, it is shown that the driving process led to the formation of a remoulded chalk annulus around the piles, but a thicker remoulded zone was found in front of the strain gauge protection. It is not surprising that the presence of a softer

remoulded annulus of different thicknesses around the pile can have a significant effect on the initial pile response under lateral loading.

However, it is interesting to note that, by shifting the response of Pile 4 by 4.5mm, the final sections of the load displacement curve for the two 'long' piles coincide, as shown in Fig. 8. The slightly stiffer response during the final loading for Pile 4 may be related to its higher moment of inertia (*I*) by about 25% resulting from the presence of the angular protections. This suggests that when the disturbed zone is fully compressed, the two piles behave in a similar way at large strains.

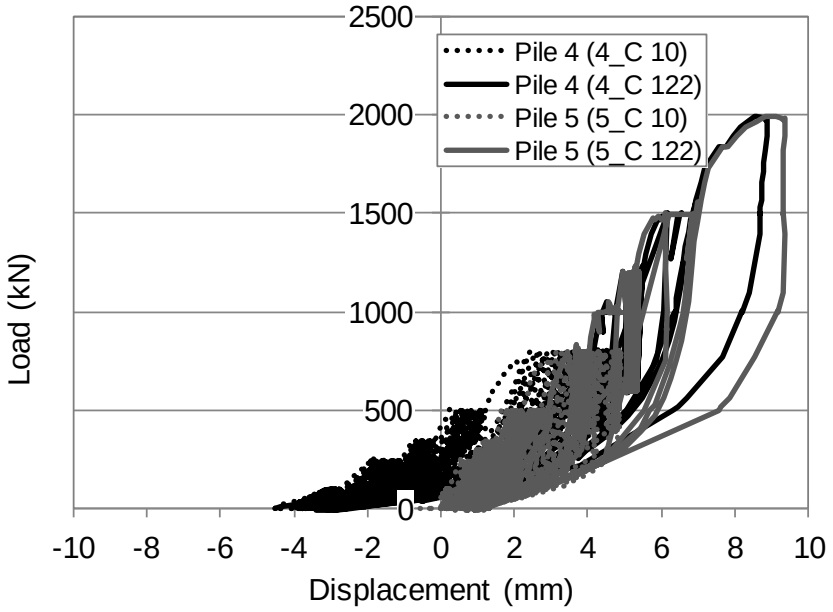

Fig. 8. Lateral Load vs Pile Head Displacement Response of 'Long' Pile 5 and Pile 4 Shifted by 4.5mm.

4.2 EVOLUTION OF PILE LATERAL STIFFNESS DURING LOADING

The existence of a remoulded chalk annulus may explain the convex shape of the initial part of the load-displacement curve observed for the instrumented piles. A clearer picture can be seen if the evolution of the tangent stiffness K_{tan} are plotted versus the pile head displacement (in a logarithmic scale) for each pile, as shown in Fig. 9. The K_{tan} values have been calculated only for the virgin (first-time) section of the loading-displacement curves. Moreover, for the piles subject to cyclic loading (Pile 3, 4 and 5), only the highest loading points of the first cycle for each cycling

sequence have been used for the K_{tan} determination in order to define as close as possible the virgin loading state.

The trends for 'short' Piles 2 and 3 (Fig. 9a) are very similar, showing an initial increase in K_{tan}, up to about 8mm displacement, followed by a subsequent drop towards zero as failure conditions are approached. The initial increase of K_{tan} is presumably related to both the compaction of the remoulded chalk annulus and the progressive closure of fractures caused by pile driving. The subsequent decrease in stiffness beyond the 8mm pile head displacement is related to incipient failure conditions within the chalk mass. The same increasing trend of K_{tan} can be observed in both tests on 'long' Pile 4, as shown in Fig.9b. In contrast, the K_{tan}-*log(d)* trend for Pile 5 (Fig.9b) shows a sharp decrease from about 750KN/mm to 400KN/mm after less than 0.2mm displacement, followed by a constant K_{tan} of 400KN/mm up to approximately 8mm displacement, followed by a decrease in K_{tan} towards zero after further displacement. Pile 4 (Fig.9b) experiences a maximum $K_{tan}$of 400kN/mm at around 11mm displacement, with a sudden reduction towards zero after further displacement, similar to Pile 5. For the sake of clarity, the interpreted trends of pile stiffness are shown as dashed lines in Fig. 9b for both Piles 4 and 5. The trends shown in Figs. 9a and 9b suggest that the additional remoulding caused by the strain gauge protection only affects lateral pile behaviour at low displacements.

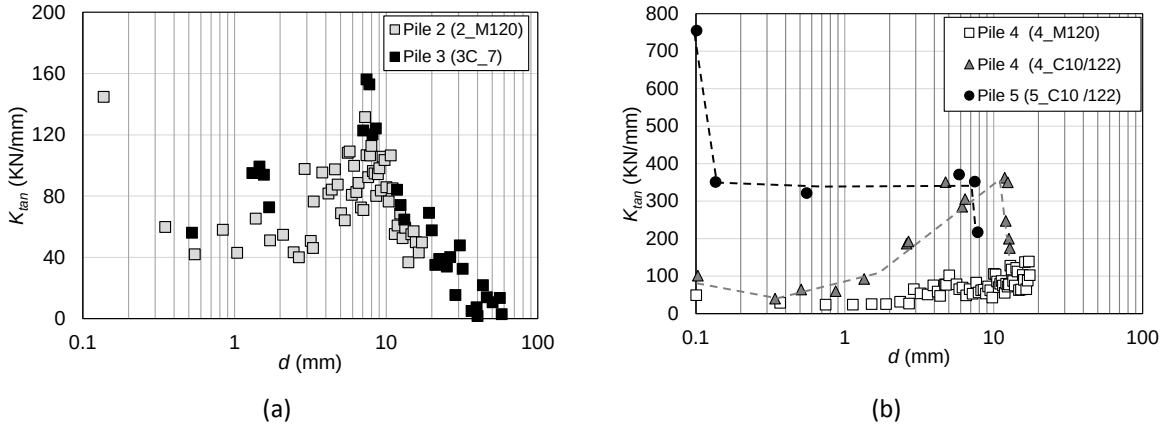

(a) (b)

Fig. 9. Tangent Stiffness versus Displacement for (a) 'Short' Piles 2 and 3 and (b) 'Long' Piles 4 and 5.

4.3 EVOLUTION OF PILE LATERAL STIFFNESS WITH TIME

The direct comparison of the load-displacement behaviour recorded for the monotonic tests carried out at approximately 7, 50 and 120 days after installation is provided in Fig.10a and 10c for Piles 2 and 4, respectively. A condition of zero pile displacement at the start of each test has been assumed. In other words, any residual displacement that existed at the end of the previous test was considered to have fully recovered in between consecutive tests. It is rather clear that the pile response seems unaffected by the time between loading and installation suggesting that "set-up" effects are not evident for this loading condition for both short and long piles. The same conclusion can be drawn by comparing the trends of tangent stiffness K_{tan} against pile head displacement (d) for the two piles in Figs. 10c and 10d, respectively.

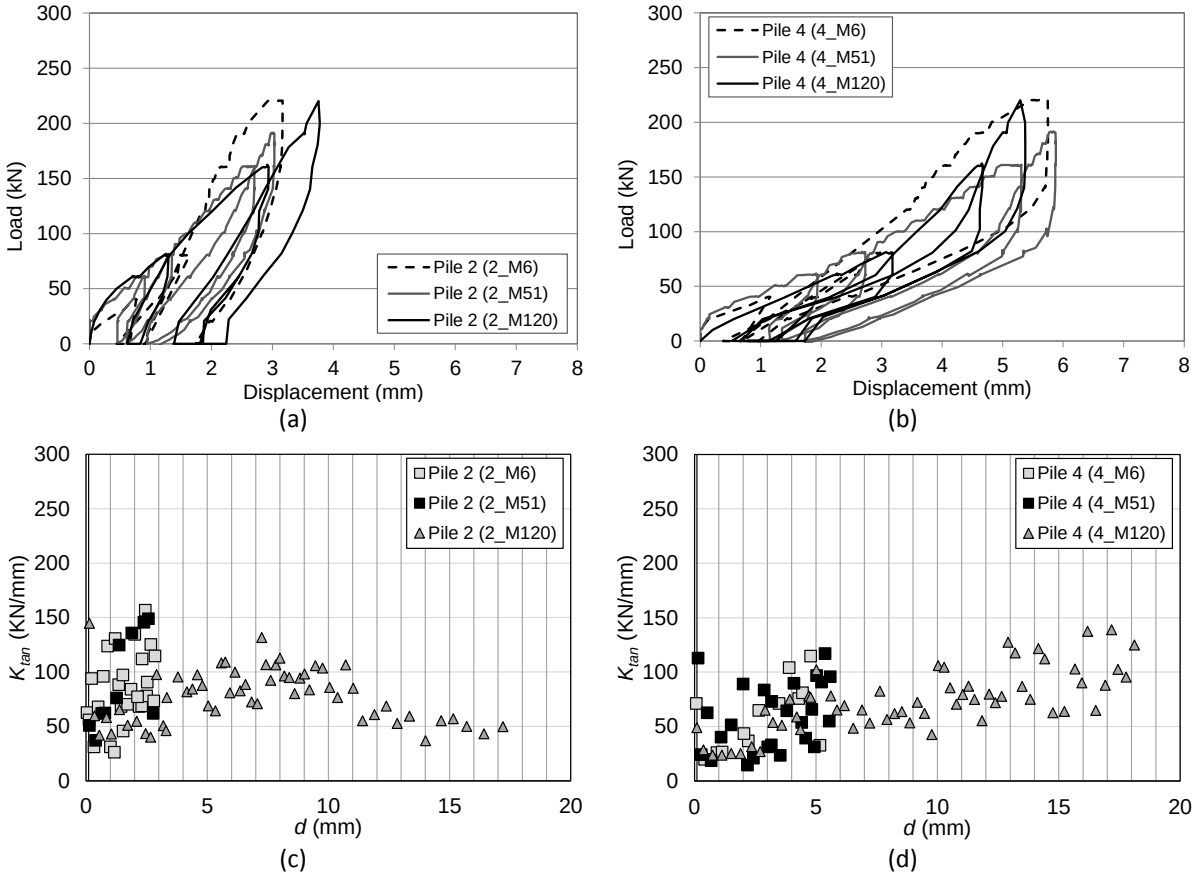

Fig. 10: Time effect on pile Load Displacement (a and b) and tangent stiffness measured (c and d) for 'short' Pile 2 and 'long' Pile 4, respectively.

5 PILE RESPONSE UNDER CYCLIC LOADING

5.1 ACCUMULATED PILE HEAD DISPLACEMENT

The accumulated pile head displacement for the generic cycle *i* (d_{acc}^{i}) is defined as:

$$d_{acc}^{i} = d^{i} - d^{1} \quad (1)$$

where d^i and d^1 are the pile head displacements on cycle no. *i* and cycle no. 1, respectively. Pile head displacements are measured at the moment of maximum load application for each cycle considered. Fig. 11 reports the trends of accumulated displacements (d_{acc}) versus the number of applied cycles during the different stages of cyclic loading for 'short' Pile 3. The accumulated displacement (d_{acc}) generally increases with maximum applied cyclic load, except for the first cyclic loading stage (0-115 kN). In this case, the progressive accumulation of displacement is likely related to the initial compaction of the remoulded chalk annulus adjacent to the pile and the closing up of fractures in the chalk mass that had been opened up during driving. However, for the second cyclic stage (0-150 kN), a much flatter response can be observed, which is probably because most of the compaction of the remoulded chalk annulus had taken place during the first stage. The trends shown in Fig.11 for the cyclic loading after stage one can be classified under two main categories:

a) For cyclic lateral load below 250kN (white filled symbols in Fig. 11), the accumulated lateral pile head displacement shows a near-linear increase with the logarithm of number of cycles (*N*) with a small increasing rate. This suggests that, up to these cyclic load levels, the pile response can be defined as 'stable'.

b) For cyclic lateral loads over 400kN (grey filled symbols in Fig. 11), the slope of the accumulated pile head displacement (d_{acc}) versus log(*N*) is progressively increasing with number of cycles. Under these conditions, the pile lateral displacements may not converge

below some critical value if the load cycles continue, possibly causing the pile to develop excessive lateral deflections after a certain number of cycles, as suggested by Li *et al.* (2010). The increasing rate in accumulated displacements under these larger load levels points to an 'unstable' pile behaviour.

The transition between the stable and unstable conditions occurred somewhere between applied peak loads of 250kN and 400kN. This corresponds to between 11% and 17% of the ultimate lateral pile load (Q_{ult}=2346 kN; see Section 4.1). This suggests that cyclic loading with a peak load of more than 11% of the ultimate lateral resistance may eventually lead to excessive deformation over the design life of a pile, if the driving process causes substantial damage of the surrounding chalk.

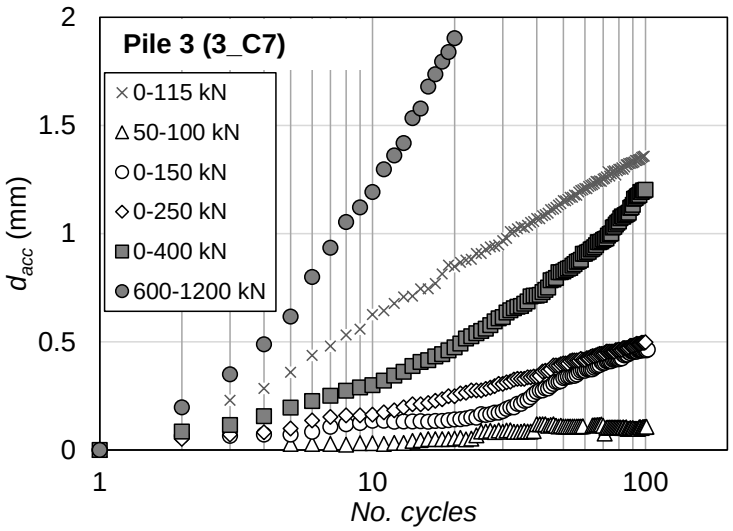

Fig .11. Accumulated Pile Head Displacement versus Number of Cycles for 'short'Pile 3 during Test 3_C7.

The measured trends of accumulated pile head displacements for 'long' Piles 4 and 5 during the first set of cyclic loading tests (4C_10 and 5C_10) are shown in Fig. 12. Direct comparison of the trends in Fig.12 a and b shows similarity of pile responses with generally larger displacements for Pile 4 at low load levels, which may be related to an increased soil disturbance during driving caused by the angular strain gauge protection system. For both these 'long' piles, the curves become steeper as the applied peak load increases, as was also observed for 'short' Pile 3.

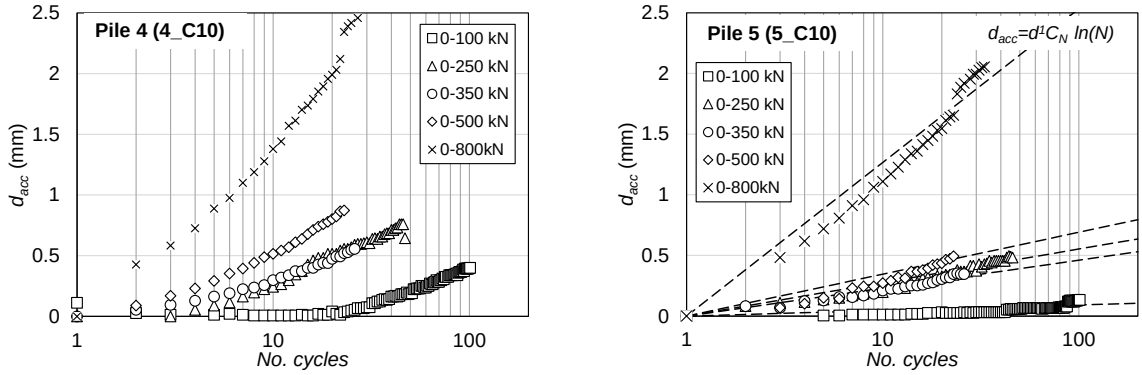

(a) (b)

Fig 12. Accumulated Pile Head Displacement versus Number of Cycles for (a) 'long'Pile 4 during Test 4_C10 and (b) 'long'Pile 5 during Test 5_C10.

The trends observed for 'long'Pile 5 (Fig.12b) appears rather linear within the range of applied number of cycles. As suggested by Verdure *et al.* (2003), the accumulated pile head displacement can be described by a logarithmic function with the number of cycles:

$$d_{acc} = d^1 C_N \ln(N) \quad (2)$$

where C_N is a non-dimensional coefficient depending on the cyclic amplitude. Comparison between experimental data and Eq.(2), using best-fit values for the coefficient C_N, is provided in Fig. 12b. The plot of the value of the slopes ($d^1 C_N$) for Eq.(2) versus the applied peak loads in Fig. 13 shows a gentle rather linear increase up to 500 kN and then a sharper increase toward the 800kN load. While these conclusions are limited by the relatively small number of applied cycles (about 20) at 800kN, this data suggests that there may be a change of pile response between 500 and 800kN applied peak load, with the possibility of the pile developing excessive lateral displacement above a certain load threshold, similarly to 'short'Pile 3.

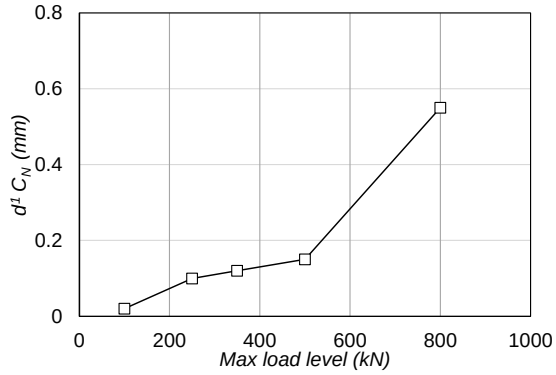

Fig 13. Trend of $d^1 C_N$ versus the Applied Peak Load for 'long'Pile 5 using data from Test 5_C10.

Further trends of accumulated pile head displacements versus number of cycles for the 'long' Piles 4 and 5 are presented in Fig. 14 for the second set of cyclic tests (4_C122 and 5C_122). For both piles the accumulated displacements are much smaller than in the previous set of cyclic tests (compare with Fig.12) as a consequence of previous loading. However, an increase in displacement accumulation rate is noticeable for the cyclic sequence beyond the maximum load applied in the previous cyclic testing campaign (>800kN). Also, a rather small accumulation rate of displacement can be observed for those cyclic loading stages which were not completely unloaded to zero (400-800kN and 600-1200 kN indicated by grey filled markers in Fig. 14).

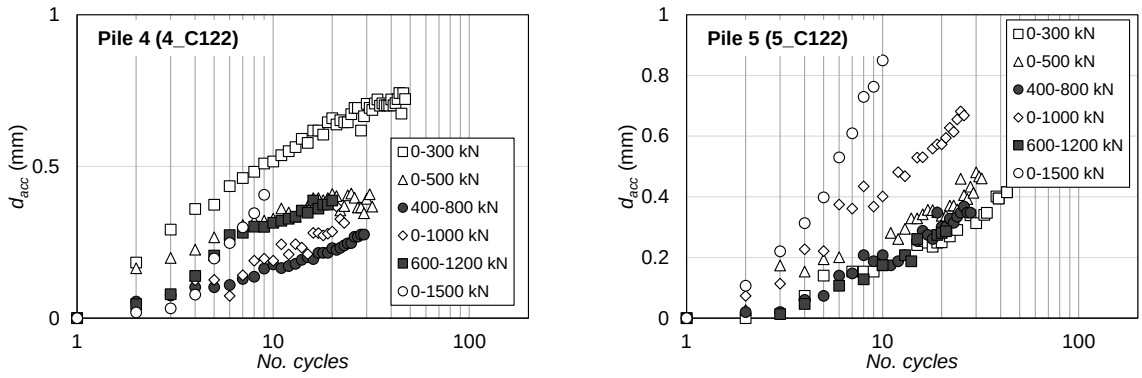

(a) (b)

Fig 14. Accumulated Pile Head Displacement versus Number of Cycles for (a) 'long'Pile 4 during Test 4_C122 and (b) 'long'Pile 5 during Test 5_C122.

5.2 PILE LATERAL STIFFNESS DURING CYCLIC LOADING

The pile secant lateral stiffness (K_{sec}) for each loading cycle is defined here as the ratio between increment in lateral load (ΔF) and pile head displacement (Δd) measured during the loading part of the considered cycle:

$$K_{sec} = \frac{\Delta F}{\Delta d} \quad (3)$$

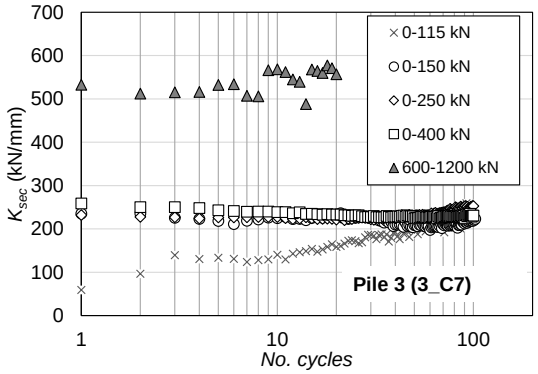

Fig.15 Pile Secant Lateral Stiffness (K_{sec}) versus Number of Cycles for 'short' Pile 3 during Test 3_C7.

The evolution of the values of the secant stiffness K_{sec} for the 'short' Pile 3 are proposed in Fig.15. For the first applied cyclic loading set (0-115 kN), K_{sec} gradually increases towards a final value of about 220 kN/mm after about 100 cycles. This may be due to a consistent compaction of the remoulded chalk annulus and closing of fractures. For all the other cyclic loading sets below 400kN, the secant stiffness initially decreases slightly with number of cycles to approach a rather similar value as measured during the initial loading set (0-115kN). A slight increase in stiffness can also be detected towards the end of the cyclic stage after about 70-80 cycles. It should be noted that the stiffness for the cyclic stage 600-1200kN is relatively high because the pile was not unloaded to zero.

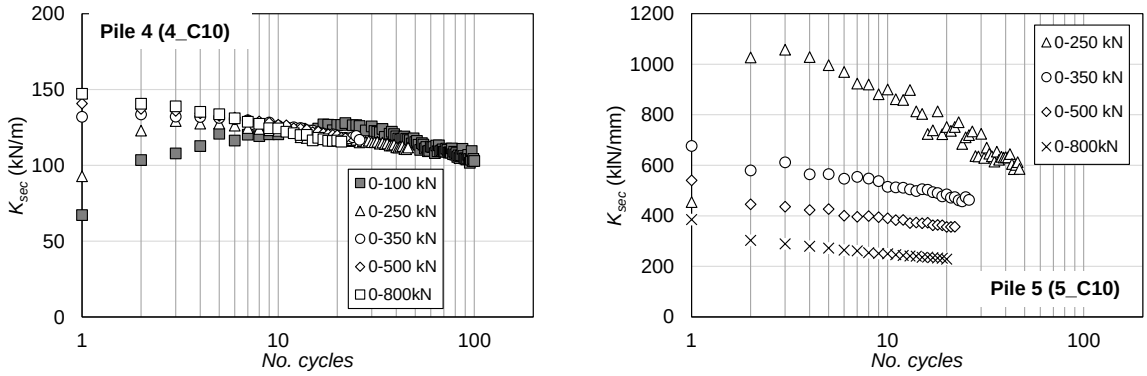

(a) (b)

Fig. 16 Pile Secant Lateral Stiffness (K_{sec}) versus Number of Cycles for (a) 'long'Pile 4 during Test 4_C10 and (b) 'long'Pile 5 during Test 5_C10.

The evolution of the pile secant stiffness K_{sec} for the 'long' Piles 4 and 5 during tests 4_C10 and 5_C10, respectively, is presented in Fig. 16. The secant stiffness, K_{sec}, for Pile 4 appears to be lower than for Pile 5 because of the additional disturbance caused by the strain gauge angular protection. For Pile 4, during the initial set of cycles (0-100kN), the secant stiffness increases significantly up to approximately the 30th cycle, which again can be related to the progressive compaction of the annulus of remoulded chalk around the pile and closing of fractures during cycling. After the 30th cycle approximately, a decrease in stiffness is observed which may be related to some degradation of the chalk mass or the formation of a gap between the pile and the chalk due to the further closure of fractures within the chalk mass. For higher cyclic load levels, a general decrease in stiffness with number of cycles can be observed. For non-instrumented 'long' Pile 5, the secant stiffness K_{sec} generally decreases with increasing load level. There is also a common decreasing trend of the stiffness with the number of cycle, which can again be related to chalk degradation or pile-chalk gap formation.

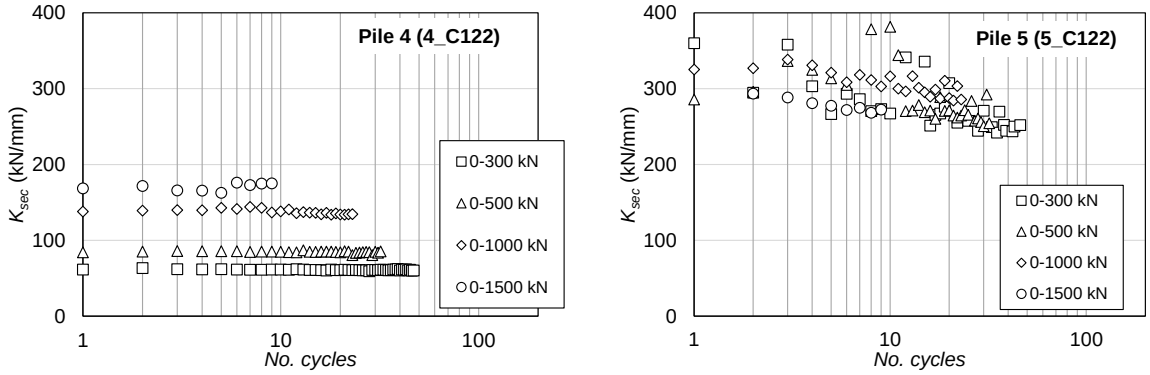

Fig. 17 Pile Secant Lateral Stiffness (K_{sec}) versus Number of Cycles for (a) 'long'Pile 4 during Test 4_C122 and (b) 'long'Pile 5 during Test 5_C122.

The pile secant stiffness K_{sec} for Piles 4 and 5 during the cyclic tests 4C_122 and 5C122 are reported in Fig.17. Pile 4 shows a general increasing trend of stiffness with the cyclic load level but there are hardly any visible change during the cyclic stage (Fig.17a). Regarding Pile 5, for the sets of load cycles where the peak load is equal to or smaller than the maximum peak load previously applied during test 5_C10 (i.e. 0-300kN and 0-500kN), the measured pile secant stiffness (Fig. 17b) is about half the corresponding one measured in the previous cyclic test, which suggests progressive degradation of chalk or formation of a pile-chalk gap. Furthermore, each stiffness measured during test 5C_122 are of similar magnitude or lower than the stiffness measured for the higher load level in the previous test 5_C10, suggesting the occurrence of irrecoverable chalk degradation or gap formation (Zhang *et al.*, 2011).

5.3 CHANGE OF SHAPE OF FORCE-DISPLACEMENT LOOPS

The evolution of the load-displacement response under cyclic loading for Pile 5 during Test 5C_10 is shown in Fig. 18 for the six cyclic sequences applied and defined in Table 3. Under low loading conditions (0-100kN), the hysteresis loop shows a general rightward shift due to the progressive accumulation of plastic pile head displacements but has no significant change in shape. A different scenario can be observed when the amplitude of the applied cyclic loading increases as shown in Fig. 18b to Fig. 18e; the hysteresis loops undergo a progressive change in shape with increasing

cyclic load level. The reloading part of the curve evolves from a convex to a concave shape characterized by an increasing tangent stiffness with the pile head displacement level. This appears to be related to the formation of a small gap between the pile head and the chalk, which results in an initial lower stiffness which progressively increases as the pile-soil gap reduces during each reload. Similar overall pile behaviour was numerically obtained by Heidari *et al.* (2013) by considering the formation of a pile-soil gap during cyclic loading. In contrast, when the cyclic load level is maintained so that pile-chalk contact is not lost, as shown in Fig. 18f for cycles between 400-800kN, the response seems almost linear elastic with little hysteresis and a progressive rightwards shift due to plastic pile head displacement accumulation.

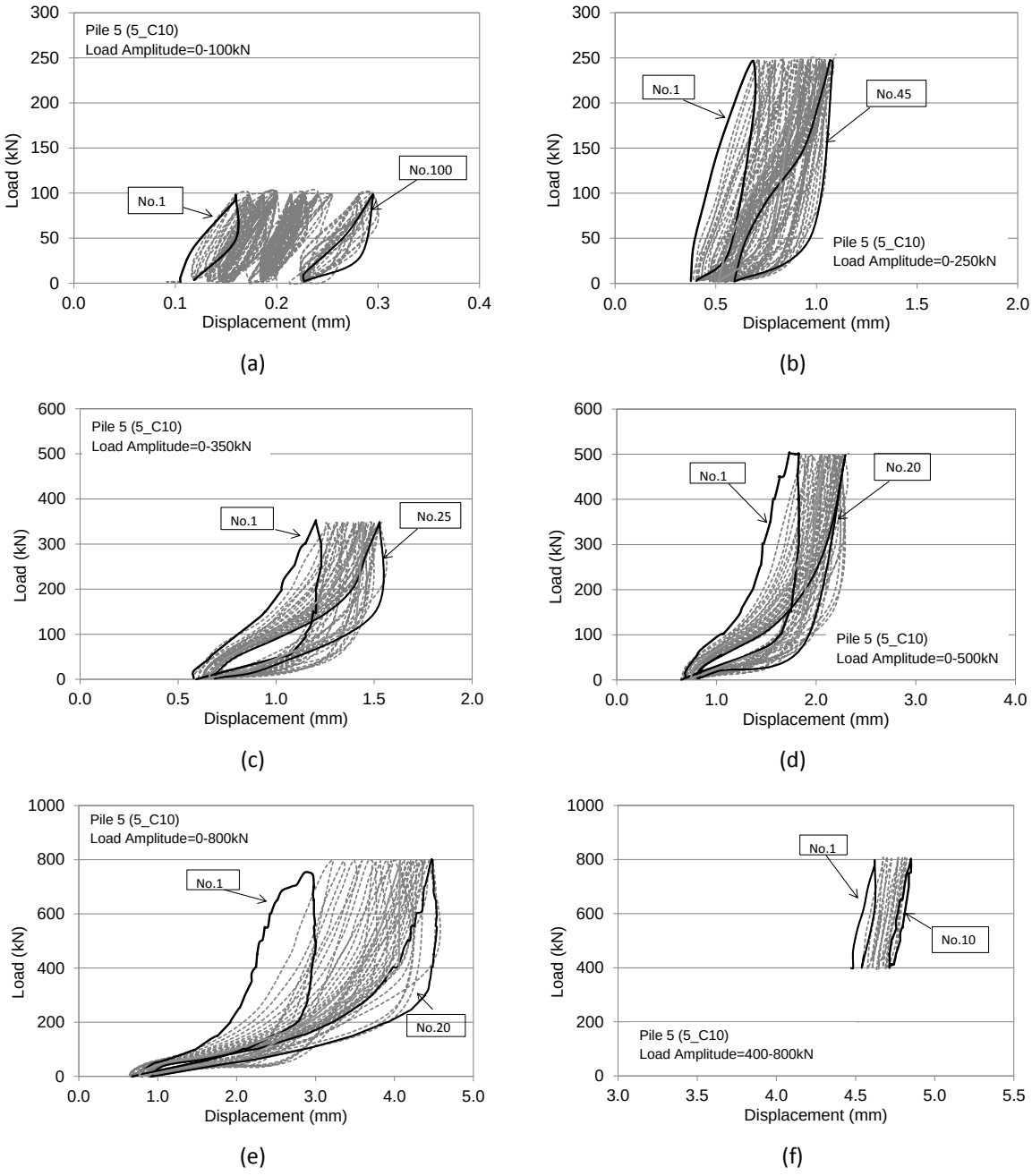

Fig.18 Evolution of Shape of Load-Displacement Loops during Cyclic Loading Test 5_C10 on Pile 5.

6 SUMMARY CONCLUSIONS

Due to the lack of available pile test data on laterally loaded piles in chalk and the difficulties faced by industry when designing pile foundation for offshore wind turbines in chalk, a set of lateral load tests on steel driven piles in low to medium density chalk was performed. Two of the four piles

tested are representative of ‘short’ rigid piles while the other two are representative of ‘long’ flexible piles.

The results of this tests campaign have been analysed in relation to the ultimate lateral load resistance, the lateral load-deflection behaviour under cyclic loading, initial stiffness variation under monotonic (including set-up effect) and cyclic loading. The main results are summarised as follows:

1. The steel channels that were welded to the outside of the piles to protect the strain gauges during pile installation, created additional chalk disturbance and had a significant effect on the initial lateral pile response. For the non-instrumented pile, only a thin annulus of remoulded chalk was created and the tests results indicate that the lateral pile response was not influenced significantly by the presence of this annulus. The non-instrumented pile is considered to be more representative of working piles.
2. Comparison of the monotonic lateral load tests carried out at different times after pile installation shows that the lateral pile response is not influenced by chalk 'set-up' effe**c**ts. This suggests that either the confined stiffness of remoulded chalk is not affected by 'set-up' or the stiffness of the remoulded annulus of chalk around the pile wall does not have a significant influence on the overall lateral behaviour of the pile.
3. For the ‘short’ piles, the envelope of the cyclic loading curve was found to be very similar to the monotonic loading curve, which suggests that the applied number and level of cyclic loading, did not affect the ultimate lateral resistance of the chalk.
4. For the ‘long’ piles, the accumulated cyclic displacement trend versus the logarithm of number of cycles (*N*) is generally linear for the range of applied load cycles. For the ‘short’ piles, the accumulated displacement was found to stabilise only when the peak cyclic load corresponds to less than 11-17 % of the ultimate monotonic lateral resistance of the chalk.

This has obvious implications for pile design. If a particular cyclic load is expected to have more around 100 cycles during the lifetime of the structure, it would be prudent to ensure that the associated peak loads do not mobilize more than 11% of the ultimate lateral resistance of the chalk at any depth

5. For the 'long' non-instrumented pile, the cyclic secant stiffness decreases with increasing peak load and load amplitude. The cyclic secant stiffness also decreases with increasing number of cycles.
6. For a 'long' pile, a subsequent reduction in cyclic peak load does not result in an increase in secant stiffness (if the pile is unloaded to zero), simply because the chalk has experienced unrecoverable plastic strain under higher loads and a gap has been created between the top of the pile and the surrounding chalk.
7. The gap between the chalk and pile that is created during cyclic lateral loading affects the shape of the load-displacement hysteresis loop. The reloading part of the curve evolves from a convex to a concave shape characterized by an increasing tangent stiffness with the pile head displacement level.

Acknowledgments

This research project was collectively sponsored by DONG Energy Power, Scottish Power Renewables, Centrica Renewable Energy, Statoil, Statkraft, Vattenfall, Fugro Geoconsulting, and Lloyd's Register.

This research was also supported and reviewed by Det Norske Veritas (DNV) and Germanischer Lloyd. The valuable and professional contribution of PMC in carrying out the pile tests is acknowledged.

7 REFERENCES

Ciavaglia F, Carey J and Diambra A (2016) Time dependent uplift capacity of driven piles in low to medium density chalk. Géotechnique Letters (in press)

Diambra A, Ciavaglia F, Harman A, Dimelown C, Carey J and Nash D.F.T (2014) Performance of cyclic cone penetration tests in chalk. Géotechnique Letters ***4*(3)**: 230-237.

Fugro Geoconsulting Limited (2012a) Onshore Geotechnical Report Field Data- St. Nicholas at Wade, Kent, UK. Report. D34001-1.

Fugro Geoconsulting Limited (2012b) Laboratory Testing Report- St. Nicholas at Wade, Kent, UK. Report. D34001-2.

Heidari M, Jahanandish M, El Naggar H, Ghahramani A (2014) Nonlinear cyclic behavior of laterally loaded pile in cohesive soil . Canadian Geotechnical Journal **51**: 129–143.

Lord JA and Davies JAG (1979) Lateral loading and tension tests on a driven cased pile in chalk. In *Proceedings of the Conference on recent developments in the design and construction of piles*, ICE, London pp.113-120.

Li Z, Haigh S K, Bolton MD (2010) Centrifuge modelling of mono-pile under cyclic lateral loads. In *7th International Conference on Physical Modelling in Geotechnics*, Zurich, vol. 2, pp.965-970.

Lord JA, Clayton CRI and Mortimore RN (2002) Engineering in Chalk, Construction Industry Research and Information Association (CIRIA). Report C574, London.

Mortimore R N (2007) Chalk pit experimental site: chalk core logging. ChalkRock Ltd, Lewes, UK Document 12, pp. 1–11.

SEtech (2007) Thanet Offshore Wind Farm, Trial Site Investigation. Document 8564/1.

Terzaghi K, Peck RB, Mesri G. Soil mechanics in engineering practice. John Wiley & Sons; 1996 Feb 7.

Verdure L, Granier J and Levacher D (2003) Lateral cyclic loading of single piles in sand. International journal of physical modelling in geotechnics **3**: 17-28.

Zhang C, White D and Randolph M (2011) Centrifuge Modelling of the Cyclic Lateral Response of a Rigid Pile in Soft Clay. Journal of geotechnical and geoenvironmental engineering, ASCE **137(7)**: 717-729.